JOURNAL OF PROPULSION AND POWER
Vol. 9, No. 5, Sept.-Oct. 1993

Plasma Detachment from a Magnetic Nozzle

E. B. Hooper*
Lawrence Livermore National Laboratory, Livermore, California 94551

Magnetic nozzles are used to convert plasma pressure into directed flow, thereby providing thrust for propulsion. The detachment of the flow from the magnetic field must be highly directed or the thrust efficiency will be low. A simple model of flowing, cold plasma in an axisymmetric nozzle is considered to determine the fundamental physics and scaling of separation in the limiting case that it is determined by plasma inertia. Ion and electron motions are coupled by the ambipolar electric field. In the limit of negligible meridional electric current, separation from the field is determined by the hybrid (electron-ion) Larmor radius evaluated at the initial magnetic flux and flow velocity. It is shown that the detachment is thereby significantly constrained, but that significant improvement can be obtained if electric currents can flow across the magnetic field either in walls or as plasma currents, or if dissipative effects are sufficiently strong.

Nomenclature

a = current loop radius
$\boldsymbol{B}$ = magnetic field
B_z = axial magnetic field
$\hat{\boldsymbol{b}}$ = unit vector along magnetic field
$\boldsymbol{E}$ = electric field
E_e = electron energy
$E_\perp$ = electric field component perpendicular to B
e = electric charge (magnitude)
$\hat{\boldsymbol{e}}$ = curvilinear unit vector
$\hat{\boldsymbol{e}}_\psi$ = unit vector perpendicular to the magnetic flux surface
G = scaling parameter
$\hat{\boldsymbol{h}}$ = unit vector ($\hat{\boldsymbol{e}}_\psi \times \hat{\boldsymbol{\theta}}$)
$\boldsymbol{j}$ = electric current
$j_\parallel$ = current along magnetic field
$j_\perp$ = current across magnetic field
M_i = ion mass
m = particle mass
m_e = electron mass
n = plasma density
q = charge
R_c = magnetic field radius of curvature
R_m = magnetic field scale length
r = radial coordinate
r_0 = initial radial coordinate
s = distance along magnetic field
T_e = electron temperature
t = time
$\boldsymbol{u}$, u = flow velocity
$\boldsymbol{u}_E$ = $\boldsymbol{E} \times \boldsymbol{B}$ drift velocity
u_θ = azimuthal velocity
u_ψ = velocity in the $\hat{\boldsymbol{e}}_\psi$ direction
u_0 = initial flow velocity
$\boldsymbol{v}$ = normalized flow velocity
$\boldsymbol{v}_e$ = electron drift velocity
$v_{e\perp}$ = electron drift velocity perpendicular to the flux surface
z = axial coordinate
$\hat{\boldsymbol{\theta}}$ = unit vector in azimuthal direction
Φ = electric potential
$\Psi(r, z)$ = magnetic flux at r, z
Ψ_0 = initial magnetic flux at r_0, z_0
ψ = Ψ/Ψ_0
$\tilde{}$ = indicates meridional components

Presented as Paper 91-2590 at the AIAA/SAE/ASME 27th Joint Propulsion Conference, Sacramento, CA, June 24–26, 1991; received Aug. 9, 1991; revision received Sept. 15, 1992; accepted for publication Dec. 10, 1992.

*Special Assistant for Science and Technology, Magnetic Fusion Energy, L-637. Member AIAA.

I. Introduction

IT is relatively straightforward to design a magnetic nozzle for a plasma thruster that will accelerate the plasma down a magnetic field gradient, converting pressure into directed flow. The nozzle may be pictured as "tubes" of magnetic field, corresponding to constant magnetic flux. A decreasing magnetic field corresponds to an increasing area of the flux tube, shaped similarly to a conventional rocket nozzle. However, unlike a conventional nozzle, the magnetic field fills all space with the field lines generally closing on themselves. The plasma will not necessarily detach (separate) from the curved field, in which case it is effectively "tied" to the thruster and generates no thrust. If it does separate, the result will be a plasma thruster (rocket) capable of the exhaust velocity potentially optimal for interplanetary travel, typically 0.3–1 $\times$ 10^5 m/s. Therefore, separation with a highly directional thrust is the sine qua non issue; without it a thruster will be unusable.

Here, a simple model in which plasma is formed with an initial flow velocity along the field and down the magnetic gradient is analyzed. Detachment of the plasma from the magnetic field in a directed flow is evaluated in the limit that it is determined by inertia. Several effects which are important in actual devices are neglected, including ionization, the effects of the plasma acceleration down the field gradient, and effects such as collisional dissipation, instabilities, and electric currents flowing across the magnetic field outside the region analyzed. The model is particularly relevant to plasmas generated by radio-freqency heating or other means with little electric current across the magnetic field.

This analysis yields a fundamental, lower limit to the separation which will occur in an actual device; it also describes the physics in the absence of dissipation and provides guidance to magnetic geometries to optimize the separation. Furthermore, the results provide a framework in which to examine the effects of neglected mechanisms.

It is important to emphasize that the present calculation yields a minimum to the separation. Detachment can be increased, e.g., by magnetic fields which maximize the nonadiabatic motion of the ions and electrons in the plasma. However, as will be seen, the controlling factor is the motion of the electrons which is adiabatic to very high energy. Roughly, significant nonadiabatic effects require the ratio of gyroradius (in terms of the electron energy) to magnetic field scale length to be of order unity. Thus, $r_e/R_m \approx 2.4 \times 10^6 E_e^{1/2}/BR_m$ with

E_e in eV, B in T, and R_m in m; at 100 eV and 0.001 T, a magnetic field scale length of 2 cm is required. Forcing the electron motion to be nonadiabatic is generally very difficult.

Dissipation, either by collisions or by turbulence, is more likely to be important in an actual device. Both mechanisms are highly sensitive to the details of the plasma flow and thermal conductivity along the magnetic field. For Coulomb collisions, e.g., the limiting cases of isothermal and adiabatic flow yield very different results. The plasma density n, scales as $nu/B \approx$ const, so that n drops rapidly as the plasma expands in the magnetic nozzle. The electron collision frequency varies as $nT_e^{-3/2}$, so for isothermal flow the collision frequency drops rapidly downstream. In the adiabatic limit, however, the collision frequency is constant throughout the flow for a ratio of specific heats = 5/3. The actual flow lies between these limits, and may be further complicated by nonisotropic electron temperatures; consequently, the effects of Coulomb collisions must be analyzed in the context of measurements or detailed modeling of the entire flow. Such effects are consequently not included in the present work.

The conditions for detachment from the field are applied to the simple case of the field generated by a loop of current. As one would expect, the detachment is severely limited by the electrons. In fact, the usable fractional area of the loop is quite small, 4% for one case considered in the analysis. This then is the minimum effective area for this simple field. As discussed, dissipation and geometric optimization may significantly increase the useful area of the nozzle.

II. Definition of the Problem

Consider the flow of plasma in a diverging magnetic nozzle. For normal plasma conditions, the plasma is magnetized and, except for drifts, can only deviate from the field by a Larmor radius. As the field weakens, however, the ion Larmor radius becomes large enough that ions are effectively unmagnetized and can cross the field lines. The electrons remain magnetized and, assuming that magnetic flux surfaces are well defined, the electric fields generated to assure quasineutrality will generally prevent the plasma from deviating strongly from the flux surfaces.

Consistent with the assumptions made in some thruster literature,[1,2] we assume that there is no cross-field electric current in the meridional plane. (Electric current is allowed to flow in the azimuthal direction.) The consequences of this constraint are evaluated a posteriori, and it is shown to be consistent with insulating boundary conditions; i.e., it is valid if no current flows outside the analyzed region. Therefore, our purpose in the analysis is to determine the resulting separation, recognizing, however, that in actual devices this approximation may be violated, e.g., by currents in metal walls or by currents due to an electrical discharge. Such effects would enhance the separation over that determined here.

Kosmahl[1] and Sercel[2] have integrated the equations of plasma flow, including a simplified pressure term. The conditions for the calculated separation are not clear from their works; a central goal here is to clarify them.

We first consider a very simple model that demonstrates the scaling associated with the flow. Take the magnetic field to be axisymmetric. Consider the limit in which the ions are unmagnetized, i.e., they have sufficient energy that their Larmor radius (defined in terms of their flow velocity, u) is large compared with scale lengths of interest. We take the electrons to be fully magnetized and to respond to forces in the drift approximation.[3] Because the electron Larmor radius is small, their flow lies nearly on the magnetic flux surface. Consequently, in order to prevent charge separation, a transverse electric field develops that approximately balances the centrifugal force seen by an ion moving along the magnetic field:

$$E_\perp \approx (M_i u^2/R_c) \tag{1}$$

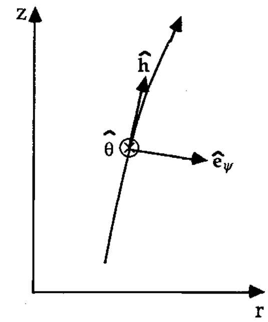

Fig. 1 Unit vectors along and across the magnetic flux surface. If the magnetic field has no azimuthal component, the unit vector along the field, $\hat{b}$, equals $\hat{h}$.

In the approximation that the flow is nearly along the field line (with distance s), the electron drift velocity is

$$v_e \approx \left(u_E - \frac{m_e u^2}{R_c}\right)\hat{\theta} + \frac{m_e u}{eB}\hat{b} \times \frac{\partial(u_E\hat{\theta})}{\partial s} \tag{2}$$

where the $E \times B$ velocity is given by $u_E \approx M_i u^2/BR_c$. The unit vectors are shown in Fig. 1; for the present approximation we assume that the magnetic field has no azimuthal component, so the unit vector along the magnetic field is $\hat{b} = \hat{h}$. Then, the last term in the electron drift is perpendicular to the flux surface and of approximate magnitude

$$\frac{v_{e\perp}}{u} \approx \frac{m_e u}{eB}\frac{M_i u}{eB}\frac{1}{R_c^2} \tag{3}$$

To satisfy quasineutrality, the ion cross-flux velocity has the same magnitude. Thus, the electrostatic coupling of the ion and electron motions required by ambipolarity causes deviations from the magnetic flux surface that scale as a hybrid (ion-electron) Larmor radius. We will see this behavior in the more precise calculation, below.

We more generally consider steady-state plasma flow in a fluid model with zero pressure and negligible collisions. In this case, the momentum equation for each species (ion or electron) is simply

$$m\boldsymbol{u}\cdot\nabla\boldsymbol{u} = q(\boldsymbol{E} + \boldsymbol{u}\times\boldsymbol{B}) \tag{4}$$

Because the magnetic nozzle is assumed axisymmetric, the field is determined by the azimuthal component of the vector potential. Thus, we can relate $\Psi(r, z)$ to the magnetic field by

$$\boldsymbol{B} = [(\hat{\theta}\times\nabla\Psi)/r] + B_\theta\hat{\theta} \tag{5}$$

with B_θ independent of the azimuthal angle. We can now define the unit vectors shown in Fig. 1 more precisely by setting $\hat{e}_\psi = \nabla\Psi/|\nabla\Psi|$ and $\hat{h} = \hat{e}_\psi \times \hat{\theta}$.

The azimuthal electric field is zero in the laboratory frame from symmetry. Then, following several transformations, the azimuthal component of Eq. (4) can be written in the form

$$\tilde{u}\cdot\nabla(mru_\theta + q\Psi) = 0 \tag{6}$$

Here, and elsewhere, we will use the tilde to indicate the two-dimensional vector with the azimuthal component absent. Equation (6), of course, just expresses the conservation of canonical angular momentum for each species along its flow trajectory.

The remaining part of Eq. (4) can now be written as

$$\tilde{u}\cdot\nabla\tilde{u} = \frac{q}{m}(\widetilde{\boldsymbol{E} + \boldsymbol{u}\times\boldsymbol{B}}) + \frac{u_\theta^2}{r}\hat{r} \tag{7}$$

The electron and ion versions of Eqs. (6) and (7) can be combined using the quasineutral condition, $\nabla \cdot \boldsymbol{j} = 0$. The results, even in the absence of coupling to the magnetic field through $\nabla \times \boldsymbol{B} = \mu_0 \boldsymbol{j}$, are complicated. Instead, we assume local ambipolarity, $\bar{\boldsymbol{j}} = 0$; this assumption was also made in Refs. 1 and 2. In this condition, the electron and ion flow trajectories are identical except in the azimuthal direction. Electric fields develop along and across the magnetic field to constrain the velocities to be equal, as in the simplified model.

In the Appendix we show that the local ambipolarity condition will be valid if the flow boundary conditions are insulating, i.e., they do not allow cross-flux currents external to the flow region. Otherwise, current loops can exist in the flow and still satisfy quasineutrality through global ambipolarity. The condition thereby requires that the azimuthal component of the magnetic field be zero, so $\hat{\boldsymbol{b}} = \hat{\boldsymbol{h}}$; in the following we assume this unless otherwise indicated. The implications of the local ambipolarity assumption are discussed in Sec. IV, where it is shown that the breakdown of the condition leads to an enhancement of the flow separation from the magnetic nozzle. We are therefore effectively considering a limiting case.

For local ambipolarity, the electron and ion meridional velocities, $\bar{\boldsymbol{u}}$, are equal. As a result, Eqs. (6) and (7) can be solved by the method of characteristics, with the electric field found by subtracting the electron version of Eq. (7) from the ion version. Along the characteristics $dr/dt = u_r$ and $dz/dt = u_z$, the azimuthal velocity for each species is determined from Eq. (6)

$$u_\theta = \frac{q}{m}\frac{\Psi_0 - \Psi}{r} \tag{8}$$

where $\Psi_0 = \Psi(r_0, z_0)$ and r_0, z_0 is the point at which the plasma is created with zero azimuthal velocity. From Eq. (8) we see that for local ambipolarity the magnitude of the electron azimuthal velocity is constrained to be larger than the ion velocity by the ion-to-electron mass ratio:

$$m_e u_{e\theta} + M_i u_{i\theta} = 0 \tag{9}$$

(We pick the ion charge to be unity with no loss of generality.) This result occurs because the transverse $\boldsymbol{E} \times \boldsymbol{B}$ drift nearly cancels the ion curvature drift. The ion detachment from the field will be reduced and the electron detachment enhanced.

Next, eliminate the azimuthal velocity for each species from Eq (7). Substitute u_θ from Eq. (8), to obtain

$$\bar{\boldsymbol{u}} \cdot \nabla \bar{\boldsymbol{u}} = \frac{q}{m}\boldsymbol{E} + \frac{q^2}{m^2}\left[\frac{\hat{\boldsymbol{\theta}} \times \boldsymbol{B}}{r}(\Psi_0 - \Psi) + \hat{r}\frac{(\Psi_0 - \Psi)^2}{r^3}\right] \tag{10}$$

Equation (5) with $B_\theta = 0$ reduces Eq. (10) to

$$\bar{\boldsymbol{u}} \cdot \nabla \bar{\boldsymbol{u}} = \frac{q}{m}\boldsymbol{E} - \frac{q^2}{m^2}\nabla\left[\frac{(\Psi_0 - \Psi)^2}{2r^2}\right] \tag{11}$$

Define the electric potential, $\boldsymbol{E} = -\nabla\Phi$. Then, to order m_e/M_i, the potential is found by subtracting the electron and ion versions of Eq. (11):

$$\Phi - \frac{e}{m_e}\frac{(\Psi_0 - \Psi)^2}{2r^2} = \text{const} \tag{12}$$

The resulting $\boldsymbol{E} \times \boldsymbol{B}$ drift of the ions perpendicular to the magnetic flux surface will reduce their azimuthal velocity, thus constraining them [by Eq. (8)] to remain close to the surface; electrons will have an increased azimuthal velocity, resulting in a displacement from the flux surface equal to that of the ions.

The equation for the plasma flow can be found by multiplying Eq. (8) by m and adding the electron and ion versions. Then, to order m_e/M_i

$$\bar{\boldsymbol{u}} \cdot \nabla \bar{\boldsymbol{u}} = -\nabla\left[\frac{e^2(\Psi_0 - \Psi)^2}{2m_e M_i r^2}\right] \tag{13}$$

III. Separation Conditions

We see from Eq. (13) that the meridional flow is determined by an effective potential. It is convenient to write this in dimensionless variables. Define $\boldsymbol{v} = \bar{\boldsymbol{u}}/u_0$ and $\psi = \Psi/\psi_0$. Also, normalize distances to r_0, the radial position where the plasma is generated. Equation (13) becomes

$$\boldsymbol{v} \cdot \nabla \boldsymbol{v} = -\frac{G}{2}\nabla\left[\frac{(1 - \psi)^2}{r^2}\right] \tag{14}$$

where

$$G = \frac{e^2\Psi_0^2}{m_e M_i r_0^2 u_0^2} \tag{15}$$

The parameter G is typically a large number. To estimate it, suppose that where the plasma is created, B_z is approximately uniform from the axis to r_0; then the flux is $\Psi_0 \approx B_z r_0^2/2$. We have

$$G \approx \frac{1}{4}\frac{eB_z}{m_e}\frac{eB_z}{M_i}\frac{r_0^2}{u_0^2} \tag{16}$$

therefore, G is thus essentially the square of the ratio of the initial radial position to a "hybrid" Larmor radius defined in terms of the initial flow energy. For $B_z = 0.1$ T and argon ions, the electron and ion cyclotron frequencies are 2×10^{10} s^{-1} and 2×10^5 s^{-1}, respectively. We are interested in thrust (flow) velocities of about 7×10^4 m/s, and, typically, $r_0 = 0.05$ m. The result is $G \approx 8.5 \times 10^2$.

This large parameter quantifies the mechanism described in the simple model in Sec. II. As long as the (normalized) value of r is $<< G^{1/2}$, Eq. (14) requires $\psi \approx 1$; i.e., the plasma remains close to the flux surface.

Next, consider the scalar product of Eq. (14) with a unit vector, $\hat{\boldsymbol{e}}$, which may be curvilinear

$$\boldsymbol{v} \cdot \nabla(\hat{\boldsymbol{e}} \cdot \boldsymbol{v}) - \boldsymbol{v} \cdot (\boldsymbol{v} \cdot \nabla\hat{\boldsymbol{e}}) = -\frac{G}{2}\hat{\boldsymbol{e}} \cdot \nabla\left[\frac{(1 - \psi)^2}{r^2}\right] \tag{17}$$

It is useful to work with the coordinate system oriented along the magnetic field (Fig. 1), with $\hat{\boldsymbol{b}} = \hat{\boldsymbol{h}}$. Note that if the magnetic field is oriented along the z axis, the perpendicular direction is radial. Also, for unit vectors

$$\hat{\boldsymbol{b}} \cdot (\bar{\boldsymbol{u}} \cdot \nabla\hat{\boldsymbol{e}}_\psi) = -\hat{\boldsymbol{e}}_\psi \cdot (\bar{\boldsymbol{u}} \cdot \nabla\hat{\boldsymbol{b}}) \tag{18}$$

The flow along and across the flux surface is then given by

$$\boldsymbol{v} \cdot \nabla v_\parallel - v_\psi \hat{\boldsymbol{e}}_\psi \cdot (\boldsymbol{v} \cdot \nabla\hat{\boldsymbol{b}}) = -\frac{G}{2}\frac{\partial}{\partial s}\left[\frac{(1 - \psi)^2}{r^2}\right] \tag{19}$$

with s distance along the field line, and

$$\boldsymbol{v} \cdot \nabla v_\psi - v_\parallel \hat{\boldsymbol{b}} \cdot (\boldsymbol{v} \cdot \nabla\hat{\boldsymbol{e}}_\psi) = -\frac{G}{2}\hat{\boldsymbol{e}}_\psi \cdot \nabla\left[\frac{(1 - \psi)^2}{r^2}\right] \tag{20}$$

The second terms on the left side of Eqs. (19) and (20) are the curvature accelerations in the curvilinear coordinate system. For example, suppose the velocity along the field is much greater than that across; using Eq. (18) we find that the curvature term in Eq. (20) is approximately $v_{\parallel}^2(r_0/R_c)$, where R_c is the radius of curvature of the field lines; this is the centripetal acceleration. Thus, if this (centrifugal) force is sufficiently strong compared to that due to the azimuthal currents, detachment occurs.

Recall that the quasilinear partial differential equation, Eq. (17), was derived assuming flow along the characteristics. In r, z coordinates these are given by

$$\frac{\mathrm{d}v_r}{\mathrm{d}t} = -\frac{G}{2}\frac{\partial}{\partial r}\left[\frac{(1-\psi)^2}{r^2}\right] \tag{21}$$

$$\frac{\mathrm{d}v_z}{\mathrm{d}t} = -\frac{G}{2}\frac{\partial}{\partial z}\left[\frac{(1-\psi)^2}{r^2}\right] \tag{22}$$

$$\frac{\mathrm{d}r}{\mathrm{d}t} = v_r \tag{23}$$

$$\frac{\mathrm{d}z}{\mathrm{d}t} = v_z \tag{24}$$

The characteristics are those of a hybrid (electron-ion) particle moving in a potential.

The energy integral along characteristics immediately follows from Eqs. (21) and (22) or, more generally from Eq. (14):

$$v^2 + G[(1-\psi)^2/r^2] = 1 \tag{25}$$

The energy places constraints on the motion and, e.g., yields a necessary condition for the flow to separate. We solve Eq. (25) for the limiting case $v = 0$:

$$\psi = 1 \pm (r/G^{1/2}) \tag{26}$$

The plasma flow must lie between the flux surfaces defined in Eq. (26). To make this more concrete, consider the special case of flow in the field generated by a current loop. The flux follows immediately from the vector potential; except near the loop, it is well approximated by

$$\psi = \frac{r^2(1+a)^3}{[(r+a)^2 + z^2]^{3/2}} \tag{27}$$

We will use this approximation throughout space for our illustration.

Equations (26) and (27) yield z^2 as a function of r

$$z^2 = \frac{(1+a)^2 r^{4/3}}{[1 \pm (r/G^{1/2})]^{2/3}} - (r+a)^2 \tag{28}$$

This is plotted in Fig. 2 for the solution with negative sign and $a = 1.5$.

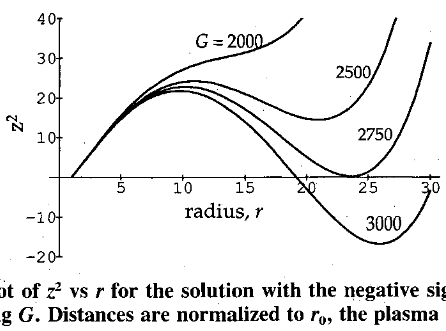

Fig. 2 Plot of z^2 vs r for the solution with the negative sign, $a = 1$, and varying G. Distances are normalized to r_0, the plasma position at $z_0 = 0$.

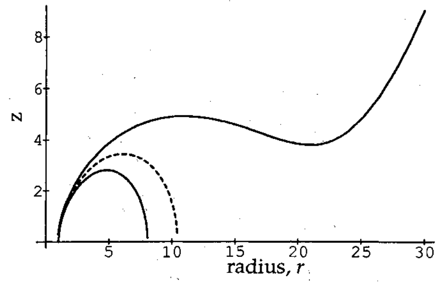

Fig. 3 Flux surface (dashed) and energetic limits to the flow for $G = 2500$.

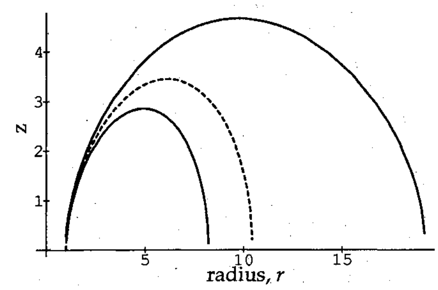

Fig. 4 Flux surface (dashed) and energetic limits to the flow for $G = 3000$.

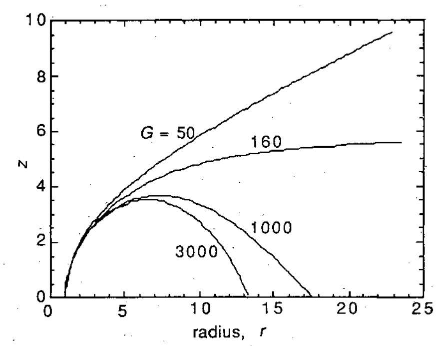

Fig. 5 Flow lines for $a = 1.5$ and various values of G.

When z^2 goes negative (and z becomes imaginary), the character of the solution changes from open to closed. Thus, there is a separatrix between flows that are energetically able to detach and those that energetically must remain closed about the current loop; for this example it occurs approximately at $G = 2750$. The limits for two cases are shown in Figs. 3 and 4. The dashed lines are the magnetic flux surfaces; the inner solid lines correspond to the positive sign in Eq. (28) and the outer solid lines to the negative sign.

Although the flow must lie between the energy limits, the dynamics may be considerably more constraining. In fact, separation will occur at rather smaller values of G than found from the energy integral. Figure 5 shows the results of integrating Eqs. (21–24) with the model flux function, Eq. (27), $a = 1.5$, and several values of G. The value $G = 160$ corresponds to the flow approaching $v_z \approx 0$ at large times.

The case in which the energy limits confine the flow to a closed region is considerably more complex than one might expect. Figure 6 shows the solution for $a = 1.5$ and $G = 3000$ for times ≤ 1 (in normalized units). The flow is confined because of the potential, but does not remain on a closed surface. In fact, it is seen to reflect off the energy limits, effectively mirroring in the magnetic field about the loop. As a consequence, there are points in space that can be reached by plasma flowing from different launching positions. The plasma conditions are obviously more complex than assumed in the present model. For example, very small collision fre-

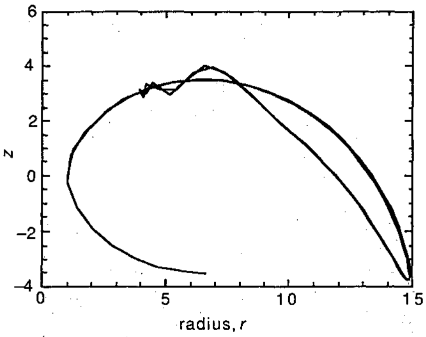

Fig. 6 Solution to the flow equations for $a = 1.5$ and $G = 3000$.

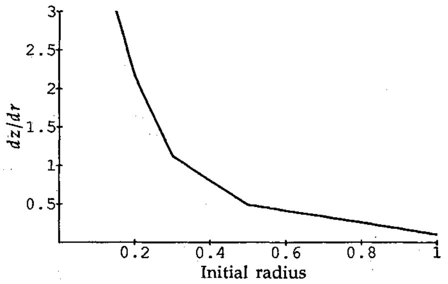

Fig. 7 Slope of the flow at large distances. Shown are results for a loop with $a = 1.5/r_0$ and $G = 100/r_0^2$.

quencies will randomize the velocity and create a pressure tensor. Also, the assumption that there is no cross-field electric current may well be violated. As we are not interested in exploring the physics of the confined plasma here, we will not analyze this further.

To examine the flow for the detaching cases, it is appropriate to consider a current loop of fixed radius (in unnormalized coordinates) and to vary r_0, the radius of plasma formation. Thus, we vary the normalized coordinates as $a \sim r_0^{-1}$ and $G \sim r_0^{-2}$. An example of the resulting angle of the detached flow at large times and distances is shown in Fig. 7. It is clear that only a small part of the aperture of the loop yields directed flow: the fractional area for flow at 45 deg ($dz/dr = 1$) or less is about $(0.3/1.5)^2 = 0.04$, with $G \approx 100/(0.3)^2 = 1100$.

It is interesting to compare these results with those of Kosmahl[1] and Sercel.[2] Both calculations include a simplified pressure model; for our purposes we use the final flow velocity to estimate G. In Kosmahl's work, argon and xenon flows are considered in solenoids of radius 0.07 and 0.13 m, and initial fields of 3 T. The final flow angle is close to 45 deg for xenon (atomic mass = 137) for the 7-cm solenoid, an initial radius of 1.4 cm, and a final flow velocity of 5×10^4 m/s, corresponding to $G = 955$. The fractional area of the aperture is about $(0.014/0.07)^2 = 0.04$.

In Sercel's work, argon (atomic mass = 40) flow is considered in a current loop of radius 0.2 m and an initial field of 800 G. The final flow angle is close to 45 deg for an initial radius of 0.035 m and a final flow velocity of 3×10^4 m/s, corresponding to $G = 920$. The fractional aperture is $(0.035/0.2)^2 = 0.03$.

Both of these calculations therefore yield low utilization of the magnet area, with directed thrust only for ions originating near the solenoid axis. This is consistent with the present results, because their basic flow assumptions are the same. It is interesting to note that Sercel gives an example of reshaping the field to enhance the directivity of the flow; the usable magnetic flux is increased, but is still small.

IV. Coaxial Nozzles

Enhancement of the detachment process can be obtained by recognizing that G, Eq. (15), is proportional to Ψ_0^2, with Ψ_0 the flux trapped inside the flux surface at the generation location. This limits the usable aperture of the magnetic nozzle as noted in Fig. 7. However, a coaxial nozzle can have reverse magnetic flux between the axis and an annular region where the plasma is generated. This can cancel flux, e.g., with a null in the plasma halfway between the inner and outer walls of the coaxial region, thereby enhancing separation. The usable area is $2\pi r_0 \delta r$, where r_0 is the radius of the annulus and δr its width. This area thus grows linearly with the radius of the coils. Furthermore, annular regions can be stacked radially, with alternating magnetic field direction in order to utilize the available space.

The detailed design of a nozzle of this type requires optimization based on the tradeoffs between directionality and sufficient expansion of the flowing plasma to extract energy from the plasma plume. This includes tailoring the curvature of the field so as to best use the centrifugal force that generates the detachment.[2]

V. Cross-Field Electric Currents and Dissipation

The local ambipolar condition need not be true anywhere in the flow. The curvature forces, Eqs. (19) and (20), are different for the electrons and ions and may result in different flow patterns. Quasineutrality only requires that the densities be equal everywhere; if it is satisfied where the plasma is generated, the condition $\nabla \cdot j = 0$ will force it to be true everywhere. Thus, in general, there will be current loops in the r, z plane, with currents (of ions) flowing across field lines balanced by currents (of electrons) flowing along the field lines. The consequence will be to somewhat relax the conditions for detachment.

In the Appendix, we show that if the boundary conditions are insulating and if there is no azimuthal component of the vacuum magnetic field, our condition is valid. In general, however, currents may flow in boundary surfaces or in the ionization and plasma acceleration region. In some devices, such as MPD arcs, such currents are generated by driving a discharge between two electrodes. In such cases, cross-flux currents will also occur in the flow region considered here.

Such cross-field currents can significantly enhance the plasma detachment from the field. Indeed, in the limit that the electrons are detached from the field lines, e.g., by a metal surface at or behind the maximum of the magnetic field, the effective value of G, Eq. (16), is decreased by the mass ratio, M_i/m_e ($=7.3 \times 10^4$ for argon). In this case, electrons will flow along field lines close to the axis of the device and "connect" with ions which detach from the field. The current loop required by $\nabla \cdot j = 0$ thus includes the ion cross-field flow. The solution of Eq. (17) with G determined solely by the ion mass will yield a good estimate of the maximum achievable separation when electrons are free to cross the magnetic field. Actual separation will lie between the two limits of G.

Design of an appropriate nozzle and plasma generation to optimize this cross-field electron flow will not be explored further here. We note, however, that this optimization may significantly enhance the performance of a rocket based on flow in a meridional (vacuum) magnetic field.

Although dissipative effects lie outside the present model, we can estimate their consequences by considering the resistive change in magnetic flux, and thus, the cross-field transport. From Faraday and Ampere's laws, we find that the flux annihilation during the flow line is given by $\Psi(t)/\Psi_0 \approx \exp[-\int \epsilon_0 \eta \omega_p^2 \, dl/u]$, where η is the resistivity, ω_p is the plasma frequency, and the integration is along the flow streamline. For coulomb collisions, $\epsilon_0 \eta \omega_p^2 \approx \nu_{ei}$ and the flux rate-of-change is just the flow-weighted average of the electron-ion collision frequency. Thus, if we assume a flow velocity of 10^5 m/s and an effective length of 1 m, we require a density of about 2×10^{15} m^{-3} at $T_e = 1$ eV, 6×10^{16} m^{-3} at 10 eV, or 2×10^{18} m^{-3} at 100 eV to significantly enhance the separation. Thus, as emphasized in the introduction, the separation due to dissipation is quite sensitive to thermal conductivity and other effects along the flow.

Instabilities and turbulence are even more difficult to address. Although instabilities are ubiquitous in plasmas, a priori quantitative evaluation of nonlinear effects is rarely successful. Consequences include enhanced resistivity, anomalous cross-field transport resulting from time-dependent breaking of the axisymmetry, and convection of plasma. The important instabilities and their consequences will be sensitive to the particular thruster physics and geometry; as a result, experimental guidance is even more necessary than for collisional effects.

As the plasma expands down the magnetic field, the ratio of plasma and magnetic field energy densities increases. The ratio of flow energy to magnetic energy is $\beta_f = nM_i u^2/(B^2/\mu_0)$: for flow along constant flux, this ratio is proportional to n^{-1}. As β_f approaches unity, there will be sufficient energy in the plasma for it to "tear" from the magnetic field. This physics, which includes significant plasma perturbation to the vacuum magnetic field and subsequent reconnection of the field lines, needs to be addressed both experimentally and theoretically.

Appendix: Current Flow Across the Flux Surface

In an axisymmetric system, a nonzero value of B_θ requires a net axial current inside the flux surface. In a magnetic nozzle, a coil carrying current to generate a vacuum B_θ would mechanically block the plasma flow, so in a useful axisymmetric nozzle any such field must be generated by plasma currents.

Plasma currents could be generated in regions outside the region of applicability of this model, especially if conducting material surfaces cross the magnetic field in the rear of the plasma generation region. In that case, currents can flow along field lines, with electrons flowing near the axis and connecting with ions which flow off axis and cross the field lines down the field; the current loop is closed in the surface.

One could also imagine that closed current loops might flow in regions of strong magnetic curvature. Such local nonzero currents could arise if ions and electrons followed different trajectories, while everywhere satisfying quasineutrality. We will show below that such currents are zero in the present model, so that $B_\theta = 0$ and local ambipolarity is self-consistent for a class of problems.

To proceed, we multiply Eq. (7) by n and add the electron and ion versions to obtain the plasma force balance equation

$$n \sum_{e,i} m\boldsymbol{u} \cdot \nabla \boldsymbol{u} = \boldsymbol{j} \times \boldsymbol{B} \tag{A1}$$

The current is therefore

$$\boldsymbol{j} = -\frac{n}{B^2} \sum_{e,i} (m\boldsymbol{u} \cdot \nabla \boldsymbol{u}) \times \boldsymbol{B} + \frac{j_\parallel}{B} \boldsymbol{B} \tag{A2}$$

The parallel current is found from the condition that $\boldsymbol{j}$ be divergence-free:

$$\boldsymbol{B} \cdot \nabla \left(\frac{j_\parallel}{B} \right) = \nabla \cdot \left[\frac{n}{B^2} \sum_{e,i} (m\boldsymbol{u} \cdot \nabla \boldsymbol{u}) \times \boldsymbol{B} \right] \tag{A3}$$

Equation (3) is a magnetic equation[4,5] which can be solved by integrating along field lines from a surface which crosses the field, e.g., at a material boundary at the back end of the source region. Thus, $j_\parallel$ can arise in two ways: 1) currents flowing from that surface and 2) those generated directly by plasma effects.

Currents through a boundary surface would typically arise if the surface were metal, so that it could short-circuit[6] the magnetic field. Alternatively, if the plasma is generated by an arc discharge, currents will be generated between the electrodes and can flow throughout the plasma. For present purposes, we assume that such currents are zero. As a result, currents in the plasma will form closed loops corresponding to the solution of Eq. (A3) with a condition of zero current at the boundary surface.

The component of current perpendicular to the magnetic field can be found from Eq. (A2)

$$j_\perp = B_h(-\beta_1' \hat{\boldsymbol{\theta}} + \beta_2' \hat{\boldsymbol{e}}_\psi) + B_\theta(\beta_1' \hat{\boldsymbol{h}} - \beta_3' \hat{\boldsymbol{e}}_\psi) \tag{A4}$$

where

$$\beta_1' = \frac{n}{B^2} \sum_{e,i} m \left(u_h \hat{\boldsymbol{h}} \cdot \nabla u_\psi + u_\psi \hat{\boldsymbol{e}}_\psi \cdot \nabla u_\psi + u_h u_\perp \hat{\boldsymbol{e}}_\psi \hat{\boldsymbol{e}}_\psi : \nabla \hat{\boldsymbol{h}} + u_h^2 \hat{\boldsymbol{e}}_\psi \hat{\boldsymbol{h}} : \nabla \hat{\boldsymbol{h}} - \frac{u_\theta^2}{r} \hat{\boldsymbol{r}} \cdot \hat{\boldsymbol{e}}_\psi \right) \tag{A5}$$

$$\beta_2' = -\frac{n}{B^2} \frac{\hat{\boldsymbol{r}} \cdot \hat{\boldsymbol{e}}_\perp}{r} \sum_{e,i} m u_\theta u_\psi \tag{A6}$$

$$\beta_3' = \frac{n}{B^2} \sum_{e,i} m \left(u_h \hat{\boldsymbol{h}} \cdot \nabla u_h + u_\psi \hat{\boldsymbol{e}}_\psi \cdot \nabla u_h + u_h u_\psi \hat{\boldsymbol{h}} \hat{\boldsymbol{h}} : \nabla \hat{\boldsymbol{e}}_\psi + u_\psi^2 \hat{\boldsymbol{h}} \hat{\boldsymbol{e}}_\psi : \nabla \hat{\boldsymbol{e}}_\psi - \frac{u_\theta^2}{r} \hat{\boldsymbol{r}} \cdot \hat{\boldsymbol{h}} \right) \tag{A7}$$

The azimuthal field, B_θ, is generated only by currents flowing in the plasma along $\hat{\boldsymbol{h}}$ and $\hat{\boldsymbol{e}}_\psi$. Furthermore, currents in the azimuthal direction are independently divergence-free, separable from those in the meridional plane, and cannot generate an azimuthal field. Thus, the only factor in Eq. (A8) which can drive a nonzero current along $\hat{\boldsymbol{e}}_\psi$, is the one proportional to β_2', arising from the $\boldsymbol{j} \times \boldsymbol{B}$ force that balances the net Coriolis acceleration associated with the flow. However, in the local ambipolar approximation used in the text, u_ψ is the same for both electrons and ions, so $\beta_2' = 0$ by Eq. (9). Current therefore flows in the azimuthal direction and, if the ratio of flow energy to field energy is large enough, will modify the magnetic field. However, in this model no cross-flux currents are generated for a zero-current boundary condition.

Acknowledgments

This work was supported by Lawrence Livermore National Laboratory under the auspices of the U.S. Department of Energy under Contract W-7405-ENG-48. The author benefited from several conversations with Joel Sercel about his work. Discussions with Jim Hammer and Don Pearlstein helped clarify the physics of the separation. Acknowledgment goes to Jeff Moller for setting up a differential equation integrator that greatly simplified calculations and plotting.

References

[1]Kosmahl, H. G., "Three-Dimensional Plasma Acceleration Through Axisymmetric Diverging Magnetic Fields Based on Dipole Moment Approximation," NASA TN D-3782, Jan. 1967.

[2]Sercel, J. C., "A Simple Model of Plasma Acceleration in a Magnetic Nozzle," AIAA Paper 90-2597, July 1990.

[3]Northrop, T. G., *The Adiabatic Motion of Charged Particles*, Interscience, New York, 1963.

[4]Kruskal, M. D., and Kulsrud, R. M., "Equilibrium of a Magnetically Confined Plasma in a Toroid," *Physics of Fluids*, Vol. 1, No. 4, 1958, pp. 265–274.

[5]Hall, L. S., and McNamara, B., "Three-Dimensional Equilibrium of the Anisotropic, Finite-Pressure Guiding-Center Plasma: Theory of the Magnetic Plasma," *Physics of Fluids*, Vol. 18, No. 5, 1975, pp. 552–565.

[6]Simon, A., "Antipolar Diffusion in a Magnetic Field," *Physical Review*, Vol. 98, No. 2, 1955, pp. 317, 318; see also *An Introduction to Thermonuclear Research*, Pergamon, New York, 1959, p. 164.

[7]Chang Díaz, F. R., private communication, NASA Johnson Space Center, Houston, TX, 1991.

[8]Gerwin, R. A., Marklin, G. J., Sgro, A. G., and Glasser, A. H., "Characteristics of Plasma Flow Through Magnetic Nozzles," Los Alamos National Lab., AL-TR-89-092, Los Alamos, NM, Feb. 1990.